TR－H－048

Estimation of Dynamic Joint Torques and Trajectory Formation from Surface EMG Signals Using a Neural Network Model

Yasuharu KOIKE　　Mitsuo KAWATO

1994. 2. 3

ATR人間情報通信研究所

〒619-02 京都府相楽郡精華町光台2-2　　☎07749-5-1011

ATR Human Information Processing Research Laboratories

2-2, Hikaridai, Seika-cho, Soraku-gun, Kyoto 619-02 Japan

Telephone: +81-7749-5-1011
Facsimile: +81-7749-5-1008

Estimation of Dynamic Joint Torques and Trajectory Formation from Surface EMG Signals Using a Neural Network Model

Yasuharu KOIKE *and* Mitsuo KAWATO

ATR Human Information Processing Research Laboratories

Address: Department 3
ATR Human Information Processing Research Laboratories
2-2 Hikaridai Seika-cho Soraku-gun Kyoto 619-02 Japan
TEL. 07749-5-1045
FAX. 07749-5-1008
e-mail. koike@hip.atr.co.jp

Abstract

The human arm has at least seven degrees of freedom: the shoulder has three, the elbow has one and the wrist has three. The number of related muscles is about thirty. Quantitative dynamical models of the arm have been playing critical roles in developing recent computational theories of motor control. Unfortunately, construction of a reliable quantitative model based just on reductionistic approach turned out quite difficult if not entirely impossible. We have focused on constructing a forward dynamics model (FDM) of human arm motion in the form of an artificial neural network while using physiological recordings of EMG signals and simultaneous measurement of movement trajectories. In previous studies we have already succeeded in: (1) estimating joint torques under isometric conditions in the horizontal plane (2) estimating four degrees-of-freedom posture in 3-D space and (3) estimating joint angular acceleration and reconstructing trajectories in the horizontal plane from surface EMG signals. In this paper, as the final step of our previous efforts, dynamic joint torques at the elbow and shoulder during movements in the horizontal plane are estimated from the surface EMG signals of 10 flexor and extensor muscles using a neural network model with a modular architecture. Moreover different trajectories are reliably reconstructed only from the arm initial condition and the EMG time course using this network and Lagrangean equations of the arm dynamics. This is the first demonstration that multi-joint movements and posture maintenance can be quantitatively and accurately predicted from multiple surface EMG signals while including complicated via-point movements as well as co-contraction of muscles.

Keyword: EMG, Forward Dynamics Model, Muscle Model, Neural Network, Modular Learning

1 Introduction

The problem studied in this paper is to find quantitative relationship between EMG signals and ensuing movements. Especially, we will construct a forward-dynamics model of human arm as an artificial neural network model while using EMG signals as control inputs. The goal is to demonstrate that two-joint arm trajectories in the horizontal plane can be reconstructed from surface EMG signals using an artificial neural network model with modular architecture.

To reveal the computational mechanisms of the CNS for motor control, quantitative dynamic arm models whose joint torques are exerted by muscle tensions have been proposed for a long time. Muscles have a spring-like behavior that depends on muscle length and activation level (Rack and Westbury 1969). Thus, dynamic arm models which include muscle tensions as control variables must be based on the spring-like properties of muscles. According to this property, Feldman proposed that posture can be determined by the equilibrium point of the length–tension curves of agonist and antagonist muscles (Feldman 1966). Recently, Feldman et al. (1990) succeeded in reproducing multi-joint trajectories just by changing the hand equilibrium point at a constant velocity. Bizzi et al. (1984) and Hogan (1984) proposed the virtual trajectory control hypothesis, and according to this hypothesis, Flash (1987) simulated multi-joint arm movements. This model assumed that the coefficients of the joint stiffness matrix were two or three times larger than the values measured by Mussa-Ivaldi et al. (1985).

The virtual trajectory control hypothesis, however, has recently begun to be doubted (Katayama and Kawato 1993, Kawato et al. 1993, McIntyre and Bizzi 1993) because the dynamic stiffness values measured during movements are smaller than or the same order as that during posture control (Bennett et

al. 1992, Gomi et al. 1992). Thus, McIntyre and Bizzi (1993) proposed a modification of the virtual trajectory control hypothesis in which CNS sends velocity as well as position information during the course of fast limb movements and succeeded in reproducing single-joint movement with a simple virtual trajectory. However, Katayama and Kawato (1991, 1993) have already examined essentially the same control scheme and found that very complicated virtual trajectories are necessary for reproducing multi-joint movements. This finding suggests that the CNS needs to compute the joint torques needed for movement and presumably the muscle activation levels needed to produce these torques. This problem is called the inverse dynamics problem. Because the dynamics of the human arm or a robotic manipulator are nonlinear, this problem is also nonlinear, and actually quite difficult to solve. But our position is that this problem can not be avoided for feedforward control (Kawato and Gomi 1992, Kawato et al. 1993, Shidara et al. 1993). To further examine these controversial computational hypotheses, quantitative arm models are essential in which the muscle tensions are explicitly represented.

There has been considerable effort to reproduce muscle tension or movements from nerve impulses or EMG in medical engineering and biomechanics as well as in physiology (Akazawa et al. 1988, Wood et al. 1989, Winters 1990, Clancy and Hogan 1991). Those studies at the lowest level constructed a muscle model which includes a spring, mass and damper. We hope that this kind of reductionistic approach will ultimately construct a good quantitative model of the musculoskeletal system step by step (i.e. muscle model, neural model, skeletal system model with variable muscle moment arms, Lagrangean dynamics model of the arm). A disadvantage of this method, however, is that some assumptions have to be made at each step since the nonlinear proper-

ties of the musculoskeletal and nervous systems are largely unknown. Our group earlier proposed a 6-muscle human arm model (Katayama and Kawato 1993) and a 17-muscle monkey arm model (Dornay et al. 1992). However, constructing reliable models is very difficult if not entirely impossible.

The relationship between EMG activity and the resulting movement has been extensively studied. Previous studies investigated the duration, magnitude, and timing of phasic EMG bursts in relation to movement amplitude, duration, and maximum speed (Gottlieb et al. 1989, Brown and Cooke 1990, Karst and Hasan 1991). It is desirable to construct a more computational and quantitative model of the relationship between EMG and movements other than those kinds of kinematic and descriptive studies to elucidate the motor control strategy of multi-joint arm movement. This is because many computational hypotheses on multi-joint arm movement control can be tested directly and reliably only on the basis of quantitative arm models.

We have been aiming at constructing a complete forward dynamics model (FDM) of the human arm by using an artificial neural network that has the ability to learn nonlinear functions which relate physiological recordings of EMG signals to simultaneous measurement of movement trajectories. We have already succeeded in: (1) estimating joint torques under isometric conditions in the horizontal plane from surface EMG signals (Koike et al. 1993), (2) estimating posture (three degrees-of-freedom at the shoulder and one degree-of-freedom at the elbow) in 3-D space from surface EMG signals (Koike and Kawato 1994a) and (3) estimating joint angular acceleration and reconstruction of trajectories in the horizontal plane from surface EMG signals (Koike and Kawato 1994b).

In the case of estimating joint angular acceleration, because the network had

to learn not only nonlinear properties of muscles, but also the dynamics of the arm, which can be described by Lagrange equation of motion, the learning was difficult. Thus, in this paper, the dynamics of the arm is explicitly described by the Lagrange equation and is not treated by the network. That is, in this paper, dynamic joint torques at the elbow and shoulder are estimated from the surface EMG signals of 10 flexor and extensor muscles using a neural network model with a modular architecture, during movement in the horizontal plane. The network itself does not deal with the arm dynamics. Instead, we wrote down the Lagrange equation of the arm dynamics which describe the relationships between joint torques and joint-angle trajectories for two-joint horizontal movement. Necessary physical parameters of the arm were measured. Therefore, the neural network learned only the nonlinear properties of muscluloskeletal systems. Finally trajectories are reconstructed using combination of the network and the Lagrange equation.

2 The model which estimates trajectories from surface EMG signals

Fig. 1 compares the information flow in the organism (A) and the computational procedure adopted in this paper (B). The following details each step.

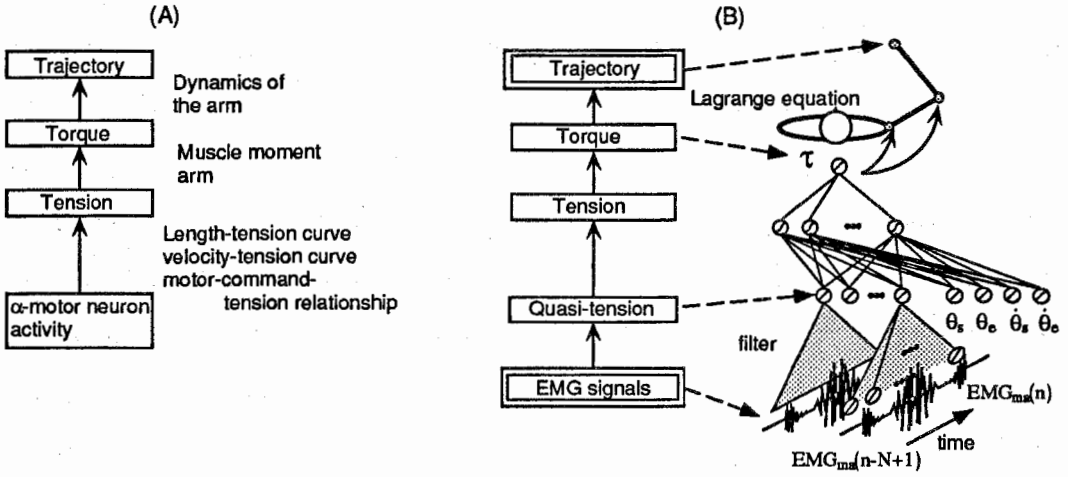

Figure 1. The comparison of the information flow in the organism (A) to the computational procedure adopted in this paper (B). In (A), control signals from the CNS are sent to each muscle via α motor neurons. The signals activate the muscles (muscle tension), the contraction causes joint torques, and then the arm moves along movement trajectories according to the arm dynamics. In (B), we can measure EMG signals and trajectory: they both have a double-line box around them. EMG signals, though temporally distorted, reflect the motor commands fed to the muscles. Since we can not measure motor neuron activity directly, though not ideal, we will treat the low pass filtered EMG activity as a substitute of the firing rate of motor neurons.

2.1 The relationship between EMG signals and quasi-tensions

Surface EMG signals are spatio-temporally folded action potentials of the muscle membranes, and involve not only descending central motor commands but also reflex motor commands generated from sensory feedback signals. There have been considerable efforts to estimate muscle force from surface EMG

signals (Basmajian and De Luca 1985, Akazawa et al. 1988, Wood et al. 1989, Clancy and Hogan 1991). From these previous studies in medical electricity and biological engineering (Basmajian and De Luca 1985), it can be expected that low-pass-filtered EMG signals reflect the firing rate of α motor neurons because high-frequency components of EMG reflect shape of the individual action potential while low-frequency components reflect the firing-frequency of motor nerve fibers; such signals are called "quasi-tensions," because they seem to be highly correlated with the true muscle tensions . In neurophysiological studies, it was found that a second-order low-pass filter is sufficient for estimating muscle forces from the nerve impulse train (Mannard and Stein 1973). The relationship between the EMG input signal and $\hat{T}$ (quasi-tension) output signal can be represented as an FIR (Finite Impulse Response) filter.

$$\hat{T}(t) = \sum_{j=1}^{n} h_j \cdot EMG(t - j + 1), \tag{1}$$

where, h_j is filter, EMG represents EMG signals, and $\hat{T}$ represents "quasi-tensions". j is the number of discrete time. EMG is actually the digitally rectified, integrated and filtered signal, which will be described in detail in section 4.4. The second-order frequency response of the filter $H(s)$ is represented as follows.

$$H(s) = \frac{\omega_n^2}{(s^2 + \zeta\omega_n s + \omega_n^2)}, \tag{2}$$

where ω_n and ζ denote natural frequency and damping coefficient, respectively. The impulse response of the function in (2) is

$$h(t) = a \times \left(exp^{-bt} - exp^{-ct}\right). \tag{3}$$

The coefficients h_j in (1) can be acquired by digitizing $h(t)$ with the given coefficients a, b and c.

2.2 Motor command and muscle tension

There exists nonlinear relationships between muscle-exerted tension and the motor commands. The muscle tension is related to motor command (firing rate) through a sigmoid function (Rack and Westbury 1969, Mannard and Stein 1973). This nonlinearity is caused not only by firing-rate-tension relationship but also by recruitment of α-motor neurons. Moreover, there are two nonlinear relationships between muscle tension and muscle length, and between muscle tension and muscle contractile velocity (Fig. 1a) (Basmajian and De Luca 1985). One is called the length–tension curve, i.e. muscle tension increases with length even if the motor command does not change. The other is called the velocity–tension curve, i.e. muscle tension decreases with contractile velocity for the constant motor command. Therefore, muscle tension can be described by the following nonlinear function of the muscle length, which is a nonlinear function of the joint angle, the contractile velocity, and the motor command:

$$\boldsymbol{T} = f\left(l(\boldsymbol{\theta}), \dot{l}(\boldsymbol{\theta}), \boldsymbol{u}\right), \tag{4}$$

where $\boldsymbol{T}$, l, $\dot{l}$, $\boldsymbol{\theta}$ and $\boldsymbol{u}$ represent muscle tension, muscle length, contractile velocity, joint angle and motor command, respectively. We call the nonlinear relationship between $\boldsymbol{u}$ and $\boldsymbol{T}$ in (4) as motor-command-tension relationship. Let us assume that the number of joints is n, and the number of muscles is k. Then $\boldsymbol{T}$, l and $\boldsymbol{u}$ are k-dimensional vectors. $\boldsymbol{\theta}$ is an n-dimensional vector. f is a k-dimensional vector function. A component of each vector is denoted as, for example, T_i $(1 \leq i \leq k)$ or θ_j $(1 \leq j \leq n)$. That is T_i is the i-th muscle tension and θ_j is the j-th joint angle.

2.3 Muscle tension and joint torque

The joint torques are determined by the product of the muscle tension and the moment arm. The distance between the joint axis and the force action line of the muscle is the muscle moment arm. The moment arm changes nonlinearly depending on the joint angle and because muscles wrap around other muscles, bones and connective tissues.

The joint torque is produced as the difference between agonist and antagonist muscle torques, which depend on the muscle tension and moment arm. It can be formulated as

$$\boldsymbol{\tau} = \sum_i \left(\boldsymbol{\alpha}_i \left(\boldsymbol{\theta} \right)^t \; T_i \left(\boldsymbol{\theta}, \dot{\boldsymbol{\theta}}, \hat{T}_i \right) \right), \tag{5}$$

where $\boldsymbol{\tau}$ and $\boldsymbol{\alpha}_i \left(\boldsymbol{\theta} \right)$ represent the joint torque and the moment arm of the ith muscle (0 for an inparticipate muscle of the considered jth joint), respectively. $\hat{T}_i$ is the ith quasi-tension. Superscript t represents the transpose of the matrix.

In this paper, we deal with horizontal planar movements of the shoulder joint (flexion-extension) and the elbow joint at the shoulder level. Then the controlled object is the two-link system comprised of the upper arm (link 1) and forearm (link 2) shown in Fig. 2. Definitions of the shoulder and elbow joint angle θ_s and θ_e are depicted in the figure. τ_s and τ_e represent shoulder and elbow joint torques. L_1 and L_2 represent the length of the link, and l_{g1} and l_{g2} represent the distance from the center of mass to the joint. Both joint angles and joint torques are defined positive in the direction of flexion. Definitions of physical link parameters are also given in Fig. 2, and they will be explained in the next section. In this case, components of vectors in (5) can be described

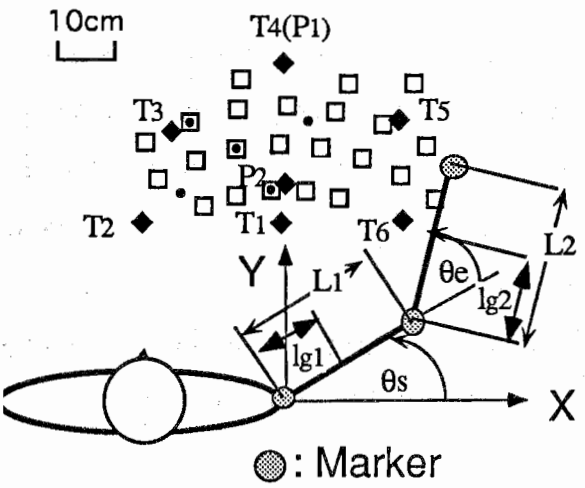

Figure 2. Experimental settings and definitions of joint angles and link physical parameters of the two-link arm model. L_1: length of upper arm, L_2: length of forearm, l_{g1}: distance from the center of mass of upper arm to the shoulder joint, l_{g2}: distance from the center of mass of forearm to the elbow joint, θ_s: shoulder joint angle, θ_e: elbow joint angle. Black circles show 5 points where the subject exerted isometric hand forces in Experiment 1. Black diamonds show the start, via- and target points of movements in Experiment 2. White squares show 23 points where postures are maintained in Experiment 3.

as follows.

$$\begin{aligned} \boldsymbol{\tau} &= (\tau_s, \tau_e)^t \\ \boldsymbol{\theta} &= (\theta_s, \theta_e)^t \\ \boldsymbol{\alpha}_i(\boldsymbol{\theta}) &= (\alpha_{is}(\boldsymbol{\theta}), \alpha_{ie}(\boldsymbol{\theta}))^t \end{aligned}$$

$\alpha_{is}(\boldsymbol{\theta})$ and $\alpha_{ie}(\boldsymbol{\theta})$ are the muscle moment arms for the shoulder and elbow joint of the i-th muscle as functions of the joint angles.

2.4 The relationship between joint torques and trajectories

We use the following dynamics equations for two-joint horizontal movements of the upper arm and the forearm.

$$\begin{aligned}
(I_1 + I_2 + 2M_2L_1l_{g2}\cos\theta_e + M_2L_1^2)\ddot{\theta}_s & \\
+(I_2 + M_2L_1l_{g2}\cos\theta_e)\ddot{\theta}_e & \\
-M_2L_1l_{g2}(2\dot{\theta}_s + \dot{\theta}_e)\dot{\theta}_e\sin\theta_e &= \tau_s \\
(I_2 + M_2L_1l_{g2}\cos\theta_e)\ddot{\theta}_s & \\
+I_2\ddot{\theta}_e & \\
+M_2L_1l_{g2}(\dot{\theta}_s)^2\sin\theta_e &= \tau_e
\end{aligned} \tag{6}$$

where τ, θ, $\dot{\theta}$, $\ddot{\theta}$ represent the joint torque, joint angle, velocity and acceleration, respectively. M_i, L_i, l_{gi}, I_i represent the mass, length, distance from the center of mass to joint, and rotary inertia around the joint for each link.

When the problem is to find the joint motion corresponding to a known sequence of input torques, the transformation (6) is referred to as *forward dynamics.* If the initial conditions: joint angles and velocities, and the control signals: joint torques from the initial time to the final time are given, then the time course of θ and $\dot{\theta}$ are obtained by numerical integration of dynamics equations (6).

When the problem is to find the joint torques corresponding to the desired time sequence of joint angles, the transformation (6) is referred to as *inverse dynamics.* In the experimental procedure of this paper, to calculate the joint torques from measured trajectories, the dynamics equations (6) are also used. In the case of forward dynamics, the information flows from the right side to the left side of (6), and in the case of inverse dynamics, the information flows

from the left to the right.

2.4.1 The physical parameters of the subject arm

The physical parameters of the arm of a human subject were calculated from the 3-D shape of the human arm. First the shape of the subject arm was scanned in a 3-D space by the Cyberware Laser Range Scanner ™. Then, assuming a uniform material with a specific gravity of 1.0, the mass, the center of mass, and the rotary inertia were calculated from the cubic volume. The same density as water is a good approximation both for soft and hard tissues. Table 1 shows the estimated physical parameters of the subject arm.

Table 1. Parameters of the human arm

		link 1 (upper arm)	link 2 (forearm)
L_i	[m]	0.256	0.315
l_{gi}	[m]	0.104	0.165
M_i	[kg]	1.02	1.16
I_i	[kgm^2]	0.0167	0.0474

3 The neural network architecture for dynamic torque estimation

Each joint torque was estimated from surface EMG signals, joint angle, and velocity using an artificial neural network model with a modular architecture as shown in Fig. 3. Here, only the network for the shoulder is shown. The modular

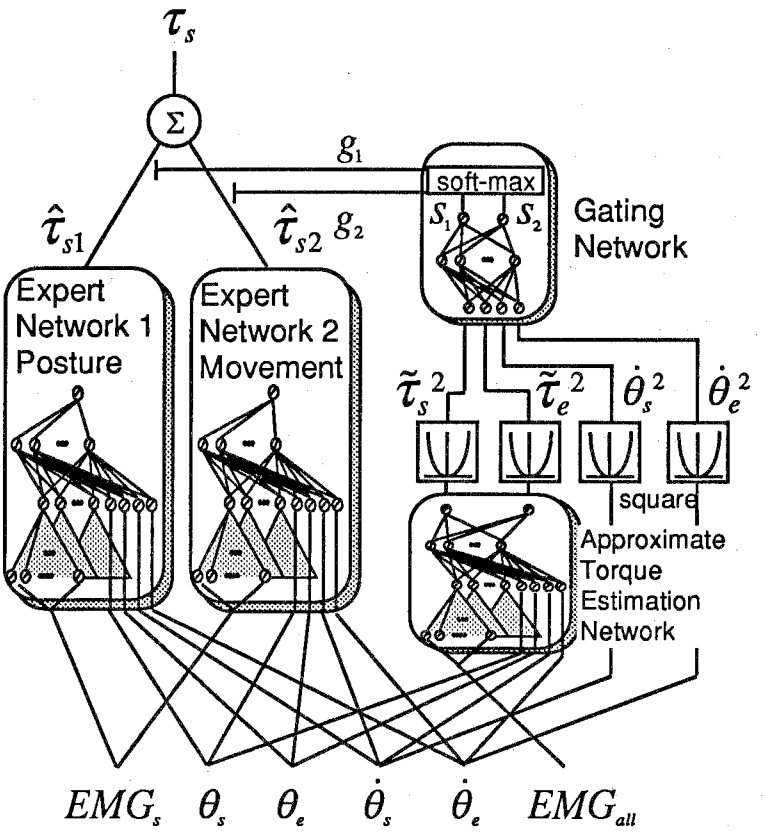

Figure 3. Structure of the artificial neural network which estimates the shoulder joint torque using a modular architecture. EMG_s is EMG signals of muscles related to the shoulder movement. EMG_{all} is EMG signals of all muscles. $\tilde{\tau}_s^2$ and $\tilde{\tau}_e^2$ are the square of the approximate torque of the shoulder and elbow respectively calculated by the approximate torque estimation network. $\hat{\tau}_{s1}$ and $\hat{\tau}_{s1}$ are shoulder joint torques estimated by the expert network 1 and 2 respectively. See (7) for g_1 and g_2.

architecture consists of two types of networks: expert and gating networks (Jacobs and Jordan 1991, Nowlan and Hinton 1991). Two modular shoulder and elbow networks were used to estimate the two joint torques respectively in order to improve the accuracy of the torque estimation. In Fig. 3, each

expert network estimated shoulder joint torque. In the case of elbow joint torque, same modular architecture was used except that expert input signals were EMG_e: EMG signals of muscles related to the elbow joint movements. The expert network 1 estimated joint torques $\hat{\tau}_{s1}$ mainly during posture control, and the expert network 2 estimated joint torques $\hat{\tau}_{s2}$ mainly during movements. This division of their roles was first attained by pre-training and further refined by the automatic modular learning algorithm explained later.

The gating network switched the expert networks by judging whether the arm moved or not. To judge whether the arm moved or not, the angular velocity was used as one of the indexes. At the start or end of a movement, the switching of the gating network based only on velocity information may be delayed, because the change in value of the velocity was small and gradual, thus difficult to be reliably detected. Therefore, torques which change faster than velocity signals, were also added as input signals to the gating network. To calculate this torque input, an approximate torque estimation network was prepared at the input side of the gating network (Fig. 3).

Each expert network consisted of a four-layer network shown Fig. 4. The first-layer inputs of this four-layer network were the EMG signals recorded from some of the ten muscles (see section 4.2) over a 0.5 second interval. The EMG signals from double joint muscles, related single joint muscles, the joint angle and the joint angular velocity of the elbow and shoulder were the expert network inputs. The number of units in the second layer was 11 for the shoulder expert network, and 9 for the elbow expert network. In a strict sense, "quasi-tension," a linearly-filtered EMG signal can not represent muscle tension. Because the FIR filter is linear, the nonlinear muscle properties found in the motor-command-tension, length-tension, and velocity-tension curves de-

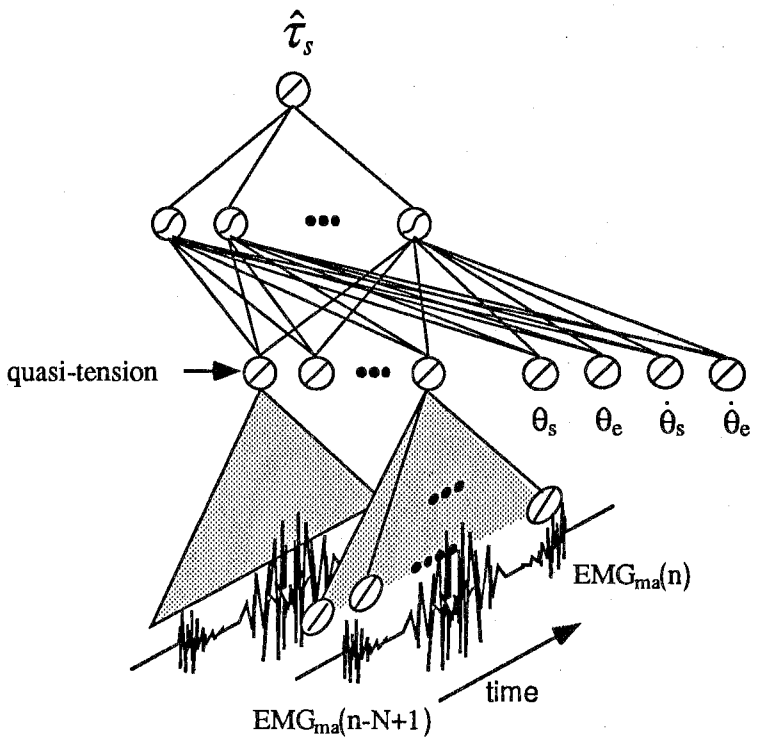

Figure 4. One of the expert neural network which estimates the shoulder joint torque. The approximate torque estimation network also has a similar structure except that it has two output units for the shoulder and elbow torques.

scribed in (4) are not represented between the first and second layers. Thus, the network learns these nonlinear properties between the second and the fourth layers. The second-layer inputs were the joint angles and joint angular velocities of the elbow and shoulder, as well as the quasi-tensions. The third layer consisted of 30 hidden units. The fourth, the output layer, estimated the joint torque. Activation functions, relating the weighted sum of synaptic inputs to the output of an artificial neuron model, of only the third layer are the nonlinear sigmoid function.

The gating network consisted of a three-layer network and the soft-max function which will be defined by (7) in the next section. The first-layer inputs were the square of each joint torque and joint velocity. Thus, the number of units in the first-layer was four (2×2). The second-layer consisted of 10 hidden units. The third, the output layer, consisted of two units which calculate s_j in (7) corresponding to two expert networks ($j = 1, 2$). Again, only the second layer units are nonlinear. The outputs of the gating network are g_1 and g_2 defined in (7).

The approximate torque estimation network also consisted of a four-layer network like the expert networks shown in Fig. 4. The first-layer inputs were the EMG signals from all the ten muscles over a 0.5 second interval. The second-layer inputs were the joint angles and joint angular velocities of the elbow and shoulder, as well as 10 quasi-tensions. Thus, the number of units in the second layer is 14. The number of units in the third layer is 30. The fourth, the output layer, consisted of two units which estimated shoulder and elbow joint torques $\tilde{\tau}_s$ and $\tilde{\tau}_e$. Again, only the third layer is nonlinear. This network had less accuracy than the expert networks, but it could provide sufficiently good information to judge whether the arm moved or not. The training method of the approximate torque estimation network is standard. The actual torques τ_s and τ_e are given as the teaching signals and the objective function is defined as the squared sum of the difference between real and estimated joint torques.

The popular back-propagation algorithm (Rumelhart et al. 1986), in conjunction with the steepest ascent method (see next subsection) was first examined. Because its rate of convergence is slow, we used the Kick-Out method (Ochiai and Usui 1994) in which learning rates are adjusted, according to the rate of increase in the objective function during the last few steps.

3.1 Modular learning

We briefly illustrate the modular learning algorithm which is proposed by Jacobs and Jordan (1991) and Nowlan and Hinton (1991), and used in this study. The j-th output of the gating network, g_j, is calculated by the following soft-max function

$$g_j = \frac{e^{s_j}}{\sum_{i=1}^{N} e^{s_i}} \tag{7}$$

where s_i is calculated from the synaptic input signals. In this study, s_1 and s_2 are outputs of two units of the third layer of the gating network as described in the previous section. N denotes the number of outputs. The total output of the modular network is as follows.

$$\tau = \sum_{i=1}^{N} g_i \hat{\tau}_i \tag{8}$$

where $\hat{\tau}_i$ is the output of the i-th expert network.

The gating and expert networks are trained to maximize the following log-likelihood function.

$$\ln L = \ln \sum_{i=1}^{N} g_i e^{-\frac{\|\tau - \hat{\tau}_i\|^2}{2\sigma_i^2}} \tag{9}$$

where, σ_i is the variance scaling parameter of the i th expert network.

The adaptation rules of the weights in the gating network are derived from the partial derivative of equation (9) by applying the chain rule.

$$\frac{\partial \ln L}{\partial s_i} = \sum_{i=1}^{N} (h_i - g_i) \tag{10}$$

where h_i is defined by the following equation corresponding to the posterior

probability.

$$h_i = \frac{g_i e^{-\frac{\|\tau - \hat{\tau}_i\|^2}{2\sigma_i^2}}}{\sum_{j=1}^{N} g_j e^{-\frac{\|\tau - \hat{\tau}_j\|^2}{2\sigma_j^2}}} \tag{11}$$

Similarly, the adaptation rules of the weights in the expert networks are derived from the partial derivative of equation (9) by applying the chain rule.

$$\frac{\partial \ln L}{\partial \hat{\tau}_i} = \sum_{i=1}^{N} h_i \frac{\tau - \hat{\tau}_i}{\sigma_i^2} \tag{12}$$

4 Experimental procedures

4.1 Experiment 1: isometric force generation

One healthy subject, 29 years old, participated in this study. The seated subject's shoulder was restrained by a harness. In the first experiment, to analyze the relationship between EMG signals and quasi-tension, the force generated at the hand under isometric conditions and surface EMG signals were measured.

His wrist was secured by a cuff and supported horizontally using the beam which was attached to a force-torque sensor. The subject was trained first to exert a hand force of about 50 % maximum. The subject exerted isometric hand forces in two different directions: forward and backward, left and right, at five different locations (θ_e, θ_s) of (30°, 110°), (40°, 80°), (50°, 90°), (60°, 100°) or (70°, 70°) indicated by the "black circles" in Fig. 2. These trials lasted for seven seconds, and were of various rates of force production. At each 5 positions, the subject tried 2 times in each direction. Thus, the rate of

the hand-force change was intentionally varied and the peak magnitude was roughly controlled.

The hand force was measured by a force-torque sensor and filtered at an upper cut-off frequency of 130 Hz by a hardware. These signals were first sampled at 2000 Hz with 12-bit resolution, and were then re-sampled at 200 Hz. The positions of the hand, elbow and shoulder were recorded at 400 Hz using the OPTOTRAK position sensing system. The shoulder and elbow joint angles were calculated from those position data. These signals were digitally filtered at an upper cut-off frequency of 10 Hz by the Butterworth filter. Then, these signals were re-sampled at 200 Hz. The shoulder and elbow joint torques were calculated from the measured hand force within the horizontal plane (two-degree-of-freedom) multiplied by the transpose of Jacobian of the coordinate transformation.

4.2 Experiment 2: movement generation

These measurements of arm positions and EMG signals were simultaneously continued during movements and maintenance of posture using the same method as Experiment 1. Again, the subject's wrist was secured by a cuff and supported horizontally. In Fig. 2, the target positions are indicated by the "black diamonds". T_1 to T_6 are starting and ending positions, and P_1 and P_2 are via points (same as Uno, Kawato and Suzuki (1989)). The subject was asked to produce five different unrestrained point-to-point movements between the five targets, i.e. $T_3 \rightarrow T_6$, $T_2 \rightarrow T_6$, $T_1 \rightarrow T_3$, $T_4 \rightarrow T_1$, $T_4 \rightarrow T_6$; movements were repeated in the opposite direction. Then, the subject made via-point movements between two targets in the horizontal plane. Two cases, $T_3 \rightarrow P_1 \rightarrow T_5$, $T_3 \rightarrow P_2 \rightarrow T_5$; were tested in both directions. The move-

ment durations ranged from about 600 ms to about 800 ms. Each of the 14 movements consisted of 10 trials. During movement, joint angular velocity and acceleration were computed using numerical differentiation. The joint torques were calculated from the trajectories using the dynamics equations (6), because dynamical torques can not be measured directly during movement.

4.3 Experiment 3: posture maintenance

In experiment 3, the subject produced co-contraction of muscles while maintaining the same posture without exertion of force at 23 points over the workspace indicated by the "white squares". Thus, the net torques generated were 0. Three trials at each point lasted for six seconds, and were of various co-contraction levels.

4.4 Muscles whose EMG activity was recorded

EMG signals were recorded from the following 10 muscles shown in Fig. 5. For flexion/extension of the shoulder joint, the deltoid-clavicular part (DLC), deltoid-acromial part (DLA), deltoid-scapular part (DLS), pectorals major (PMJ), and teres major (TEM) were measured. For double-joint muscles, the biceps-long head (BIL) and triceps-long head (TRL) were measured. For flexion/extension of the elbow joint, the brachialis (BRC), triceps-medial head (TRM), and triceps-lateral head (TRA) were measured.

The EMG signals were recorded using a pair of silver-silver chloride surface electrodes, in a bipolar configuration. Each electrode had a 10-mm diameter and were separated by approximately 15 mm. Test maneuvers were used to verify electrode placement. Each signal was sampled at 2000 Hz with 12-bit resolution. This signal was digitally rectified, integrated for 0.5 ms (EMG_{ave}

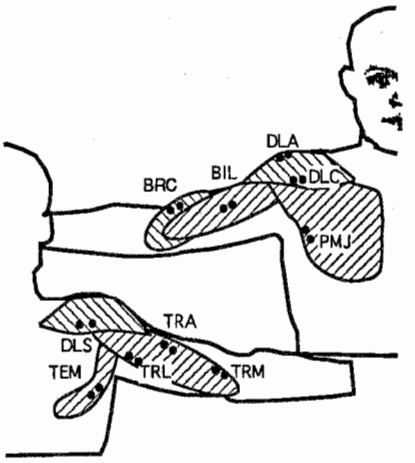

Figure 5. Electrode positions in EMG measurement. See text for muscle name abbreviations.

), sampled at 200 Hz, and finally, filtered (25-ms moving average window). This signal was denoted EMG_{ma}.

$$EMG_{ma}(t) = \frac{1}{5}\sum_{i=-2}^{2} EMG_{ave}(t-i) \tag{13}$$

The EMG_{ma} signals were used as the input signals in (1), i.e. EMG.

5 Simulation Results

5.1 Joint torque estimation using an artificial neural network model

5.1.1 Estimation of the weights between the first and second layers (filter)

To specify the relationship between EMG signals and quasi-tension, joint torques under isometric conditions measured in Experiment 1 were first esti-

mated from surface EMG signals using the simple and non-modular four-layer neural network such as shown in Fig. 4. The data from the odd numbers of 4 trials in Experiment 1 were used to train the network. Other trials were spared for a cross-validation test. The training employed 10,000 sample points for 5.0 seconds $\times$ 10 trials $\times$ 200 Hz sampling rate ($10,000 = 5 \times 10 \times 200$). The weights between the first layer and second layer after learning are shown in Fig. 6. The dotted lines for shoulder.1 and elbow.1 indicate weights obtained

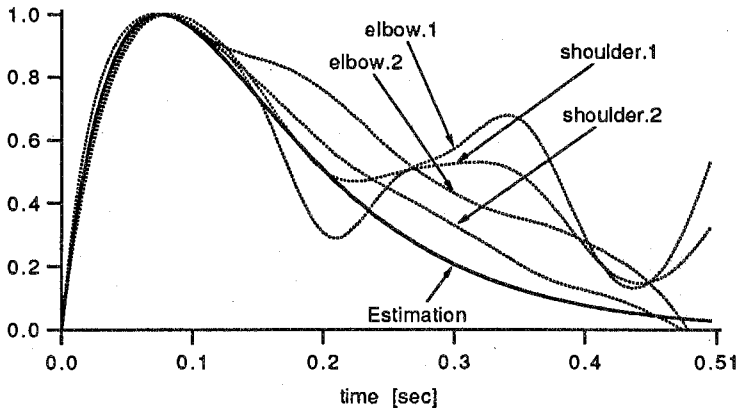

Figure 6. Impulse response of the second-order temporal filter which determines the quasi-tension from EMG. The ordinate scale is arbitrary with the peak response of 1.0.

from the previous experiment using the same subject (Koike et al. 1992). The dotted lines for shoulder.2 and elbow.2 indicate the weights obtained this time. The coefficients of (3) were estimated from shoulder.1 and elbow.1 using the least squares error method for 0.25 sec. A comparable calculation for 0.5 sec yielded weights which were less stable and variable for different joints. The solid line in Fig. 6 shows the resulting impulse response with a = 6.44, b = 10.80, and c = 16.52 in (3). Using these coefficients, the isometric torques

were estimated accurately. Because the coefficient of determination (square of the correlation coefficient between actual torques and estimated torques) for the test data was 0.897, and, moreover, shoulder.2 and elbow.2 which were obtained from the present experiment, well fitted the estimated impulse response, we can conclude that the obtained filter was reliable. The coefficients a, b, and c of the filter were fixed when the torques were estimated during movement in the next step.

Fig. 7 shows EMG signals EMG_{ma} calculated by (13), and quasi-tension $\hat{T}$ given by (1). We can see that the quasi-tension signal (smooth curve) lags

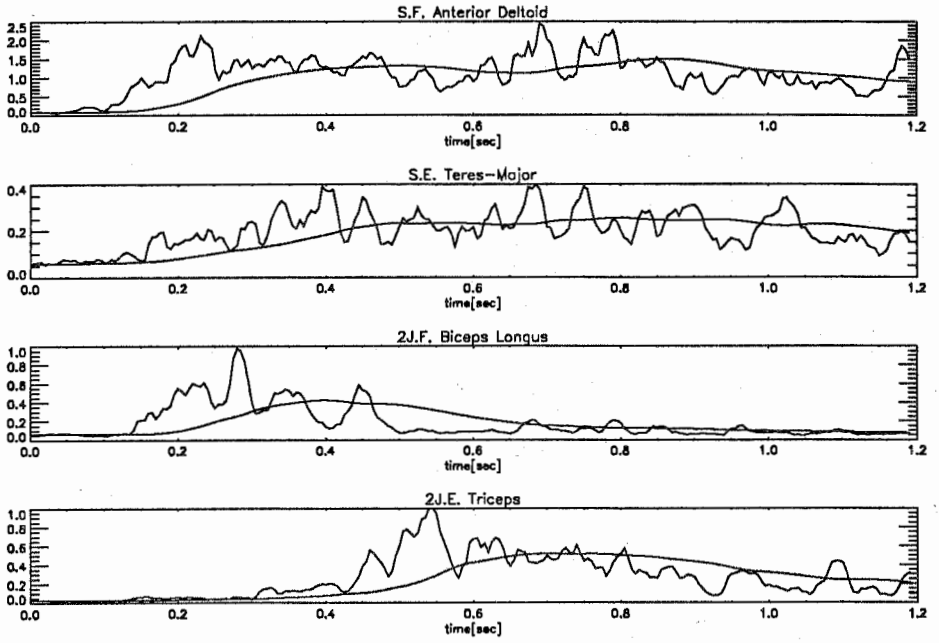

Figure 7. Measured EMG signals and quasi-tension for the four muscles (DLC, TEM, BIL, TRL).

about 100 ms behind the EMG_{ma} signals.

Prediction was made at each time step from the position, velocity and EMG data from the test set. As far as the torque is concerned, the dotted line is for the actual torque, and the solid line is for the network output. For the output of the gating network, the solid line corresponds to expert 1, and the dotted line corresponds to expert 2. Overall for test data from Experiment 2 and 3, the determination coefficient of dynamic torque is 0.887. Thus, the dynamic torques were reliably predicted by our proposed network. Expert 1's output corresponds to "posture", and expert 2's output corresponds to "movement". From the lower trace of Fig. 8, we can assert that the gating network switched the expert networks correctly for both the stopping and moving conditions.

5.2 Trajectory formation

The trajectories were calculated from the initial position and velocity, and the continuous EMG signals for point-to-point movements and via-point movements. This was done in the following recursive way.

- (Step 1)

  At each time step, the dynamic torque was predicted by the neural network model from the position and velocity values at the current time step and the past 500 msec EMG data. Then, this predicted torque is used as the control input to the dynamics equation (6).

- (Step 2)

  Numerical integration of (6) by Euler's method from the current values of the position, velocity and torque provides the next step value of position and velocity.

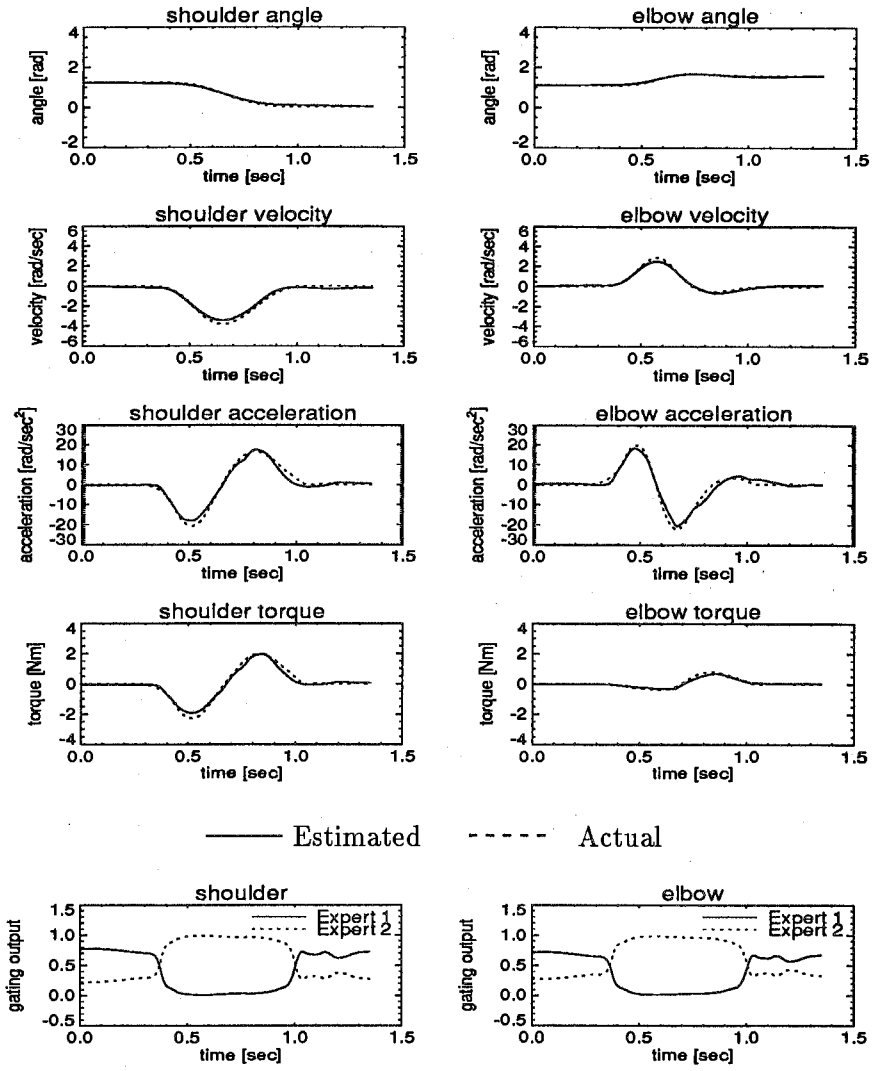

Figure 9. Joint angle (1st row), angular velocity (2nd row), angular acceleration (3rd row), and joint torque (4th row) predicted during point-to-point movement. Dotted curves show actual values and solid curves show estimated values in the upper 4 rows. The bottom row shows the outputs of the gating network. Here, solid curves show the output of the gating network for Expert 1 and dotted curves show the output of the gating network for Expert 2.

This two steps are repeated until the end of recording duration.

Fig. 9 shows one example of the simulation result of trajectory generation for $T3$ to $T6$. In descending order, the joint angle, angular velocity, angular acceleration, torque, and output of the gating network are shown. The left column corresponds to the shoulder and the right one corresponds to the elbow. In the upper 4 rows, the solid curve is the network output, and the dotted curve is the experimental data. In the bottom row, the solid curve is the output for expert 1, and the dotted curve is the output for expert 2. Similarly to the one-step prediction described before, the gating network switched the expert networks correctly for both the stopping and moving conditions. It should also be noted that at the start and end of a movement, the output of the gating network began to change in advance of the velocity change, allowing the expert network output to follow. Overall for test data shown in Fig. 10 from Experiment 2, the coefficient of determination for position data predicted from initial conditions of position and velocity and EMG time course is 0.948. Therefore, even though there was gradual cumulative error occurrence because the angle and angular velocity at the next time step were recursively calculated by summing the predicted accelerations with the current angular velocity, the trajectories were reconstructed accurately.

Fig.10 shows trajectories on the X$-$Y plane. Some trajectories were slightly different from actual trajectories, because of the error accumulation. There is, however, almost no significant error for the joint angle. This is the first demonstration that multi-joint movements and posture maintenance can be fairly accurately predicted from multiple surface EMG signals while allowing complicated via-point movements as well as co-contraction.

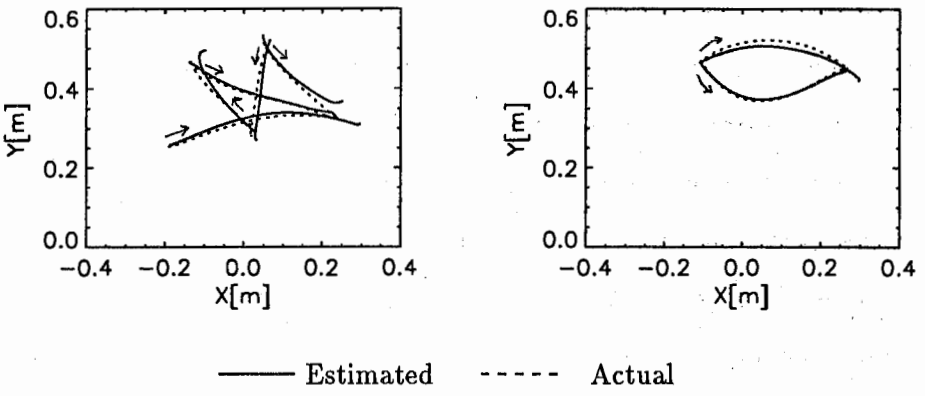

Figure 10. Calculated trajectories on XY plane. Dotted curves show actual and solid curves show estimated paths.

6 Discussion

Joint torques and then human arm movements have been estimated from surface EMG signals using a four-layer artificial neural network with a modular architecture. Particularly, we took account of the implementation of the following domain-specific knowledge. (1) the relationship between the EMG input signal and quasi-tension, (2) the dynamics of the arm, and (3) nonlinear muscle properties. To implement (1), a network was prepared to work as a temporal FIR filter between the first and second layer. In this work, we found about 100 msec lag between EMG signals and quasi-tension. Soechting and Roberts (1975) reported the natural frequency of the impulse response relating EMG to force of human muscle was 2.5 Hz. Moreover, Bawa and Stein (1976) reported that the natural frequency of the impulse response for human soleus muscle was around 2 Hz. These natural frequency corresponded to about 60 to 100 msec delay between EMG signals and muscle tension. Bennett (1993) also

pointed out the low-pass muscle property and reported about from 60 msec to about 90 msec delay between surface EMG signals and the human arm muscle tension. To implement (2), the physical parameters of the subject arm were calculated from the measured 3-D shape of the arm, and the arm dynamics were described by the Lagrange equations. Furthermore, some nonlinear properties of the musculo-skeletal system were obtained by the training of the neural network; expert networks were trained separately for training data focusing on moving or stopping to efficiently implement (3). There were some reasons for using two expert networks. From the physiological view points, the use of muscles were different depending whether the arm moves or not. When the arm was moving, the relationship between velocity and tension has to be considered. The approximate torque estimation network was added to calculate joint torques to provide the useful information for the gating network.

Until now mainly qualitative descriptions have been made regarding the relationship between movements and EMG, such as recognizing registered movement patterns from surface EMG signals (Suzuki and Suematsu 1969, Mori et al. 1992). In this paper, however, trajectories were estimated quantitatively from surface EMG signals. The constructed forward dynamics model will be served as a fundamental tool for computational study of multi-joint arm movements. Other than this scientific use, several engineering applications might also be possible. For example, by using the network, EMG signals could be used as human interface inputs to control a "virtual arm" in a virtual reality environment. A further possibility is for the motor command produced by a minimum-muscle-tension-change model (Uno, Suzuki and Kawato 1989) based on the neural network forward dynamics model to be applied to a paralyzed limb.

Regarding computational studies of motor control based on the acquired forward dynamics model, our future work includes 1) calculating of virtual trajectories to critically examine the virtual trajectory hypothesis (see Koike and Kawato (1993) for preliminary results), 2) learning the inverse dynamics model, 3) examining a minimum-motor-command-change model (Kawato 1992).

Acknowledgment

We thank Dr. F. Kishino and N. Wada of ATR Communication Systems Research Laboratories for their help in measuring the 3-D shape of the human arm. We are grateful to D.J. Ostry for his editing of the first draft of this paper. Partly supported by Human Frontier Science Program grants to M. Kawato.

References

Akazawa, K., Takizawa, H., Hayashi, Y. and Fujii, K. (1988) Development of control system and myoelectric signal processor for bio-mimetic prosthetic hand, *Biomechanism* **9**: 43–53.

Basmajian, J. V. and De Luca, C. J. (1985) *Muscles Alive*, Williams & Wilkins, Baltimore.

Bawa, P. and Stein, R. (1976) Frequency response of human soleus muscle, *Journal of Neurophysiology* **39**: 788–793.

Bennett, D. (1993) Electromyographic responses to constant position errors imposed during voluntary elbow joint movement in human, *Exp. Brain Res.* **95**(3): 499–508.

Bennett, D., Hollerbach, J., Xu, Y. and Hunter, I. (1992) Time–varying stiffness of human elbow joint during cyclic voluntary movement, *Exp. Brain Res.* **88**(2): 433–442.

Bizzi, E., Accornero, N., Chapple, W. and Hogan, N. (1984) Posture control and trajectory formation during arm movement, *The Journal of Neuroscience* **4**(11): 2738–2744.

Brown, S. and Cooke, J. (1990) Movement related phasic muscle activation. I. Changes with temporal profile of movement, *Journal of Neurophysiology* **63**(3): 455–464.

Clancy, E. A. and Hogan, N. (1991) Estimation of joint torque from the surface EMG, *Annual International Conference of the IEEE Engineering in Medicine and Biology Society* **13**(2): 0877–0878.

Dornay, M., Uno, Y., Kawato, M. and Suzuki, R. (1992) Simulation of optimal movements using the minimum-muscle tension-change model, *in* J. M. Moody, S. J. Hanson and R. P. Lippmann (eds), *Advances in Neural Information Processing Systems 4*, Morgan Kaufmann, San Meteo, pp. 627–634.

Feldman, A. (1966) Functional tuning of the nervous system with control of movement or maintenance of a steady posture.iii. Mechanographic analysis of execution by man of the simplest motor tasks, *Biophysics* **11**: 766–775.

Feldman, A., Adamovich, S., Ostry, D. and Flanagan, J. (1990) The origin of electromyograms - explanations based on the equilibrium point hypotheses, *in* J. M. Winters and S. L.-Y. Woo (eds), *Multiple Muscle Systems*, Springer-Verlag, New York, pp. 195–213.

Flash, T. (1987) The control of hand equilibrium trajectories in multi-joint arm movement, *Biological Cybernetics* **57**: 257–274.

Gomi, H., Koike, Y. and Kawato, M. (1992) Human hand stiffness during discrete point-to-point multi-joint movement, *Proceedings of Annual International Conference of the IEEE Engineering in Medicine and Biology Society* **14**: 1628–1629.

Gottlieb, G. L., Corcos, D. M. and Agarwal, G. C. (1989) Organizing principles for single-joint movements I. A speed-insensitive strategy, *Journal of Neurophysiology* **62**(2): 342–357.

Hogan, N. (1984) An organizing principle for a class of voluntary movements, *The Journal of Neuroscience* **4**(11): 2745–2754.

Jacobs, R. and Jordan, M. (1991) A competitive modular connectionist architecture, *in* J. M. Moody, S. J. Hanson and R. P. Lippmann (eds), *Advances in Neural Information Processing Systems 3*, Morgan Kaufmann, San Meteo, pp. 767–773.

Karst, G. M. and Hasan, Z. (1991) Timing and magnitude of electromyographic activity for two-joint arm movements in different directions, *Journal of Neurophysiology* **66**(5): 1594–1604.

Katayama, M. and Kawato, M. (1991) Virtual trajectory and stiffness ellipse during force-trajectory control using a parallel-hierarchical neural network model, *Proceedings of the Fifth International Conference on Advanced Robotics* pp. 1187–1194.

Katayama, M. and Kawato, M. (1993) Virtual trajectory and stiffness ellipse during multijoint arm movement predicted by neural inverse models, *Biological Cybernetics* **69**(5/6): 353–362.

Kawato, M. (1992) Optimization and learning in neural networks for formation and control of coordinated movement, *in* D. Meyer and S. Kornblum (eds), *Attention and Performance,XIV Cambridge*, MIT Press.

Kawato, M. and Gomi, H. (1992) The cerebellum and VOR/OKR learning models, *Trends in Neurosciences* **15**(11): 445–453.

Kawato, M., Gomi, H., Katayama, M. and Koike, Y. (1993) Supervised learning for coordinative motor control, *in* E. B. Baum (ed.), *Computational learning & cognition*, Society for Industrial and Applied Mathematics, Philadelphia, pp. 126–161.

Koike, Y. and Kawato, M. (1993) Virtual trajectories predicted from surface EMG signals, *Society for Neuroscience Abstracts* **19**: 543.

Koike, Y. and Kawato, M. (1994a), Estimation of arm posture in 3D-space from surface EMG signals using a neural network model, *IEICE Transactions Fundamentals.* (in press).

Koike, Y. and Kawato, M. (1994b), Trajectory formation from surface EMG signals using a neural network model, *IEICE Transactions (D-II)* **J77**(1): 193–203. (in Japanese).

Koike, Y., Honda, K., Hirayama, M., Gomi, H., Bateson, E.-V. and Kawato, M. (1992) Dynamical model of arm using physiological data, *Technical Report of IEICE NC91-146* pp. 107–114. (in Japanese).

Koike, Y., Honda, K., Hirayama, M., Gomi, H., Bateson, E.-V. and Kawato, M. (1993) Estimation of isometric torques from surface electromyography using a neural network model, *IEICE Transactions (D-II)* (6): 1270–1279. (in Japanese).

Mannard, A. and Stein, R. (1973) Determination of the frequency response of isometric soleus muscle in the cat using random nerve stimulation, *J. Physiol.* **229**: 275–296.

McIntyre, J. and Bizzi, E. (1993) Servo Hypotheses for the Biological Control of Movement, *Journal of Motor Behavior* **25**(3): 193–202.

Mori, D., Tsuji, T. and Ito, K. (1992) Motion discrimination method from EMG signals using statistically structured neural networks, *Technical Report of IEICE NC91-143* pp. 83–90. (in Japanese).

Mussa-Ivaldi, F., Hogan, N. and Bizzi, E. (1985) Meural, mechanical, and geometric factors subserving arm posture in humans, *The Journal of Neuroscience* **5**(10): 2732–2742.

Nowlan, S. and Hinton, G. (1991) Evaluation of adaptive mixtures of competing experts, *in* J. M. Moody, S. J. Hanson and R. P. Lippmann (eds), *Advances in Neural Information Processing Systems 3*, Morgan Kaufmann, San Meteo, pp. 774–780.

Ochiai, K. and Usui, S. (1994) Kick-out learning algorithm to reduce the oscillation of weights, *Neural Networks.* (in press).

Ochiai, K. and Usui, S. (Mar. 1993) Improved kick out algorithm with delta-bar-delta-bar rule, *International Conference on Neural Networks* **1**: 269–274. San Francisco.

Rack, P. and Westbury, D. (1969) The effects of length and stimulus rate on tension in the isometric cat soleus muscle, *Journal of Physiology* **217**: 419–444.

Rumelhart, D., Hinton, G. and Williams, R. (1986) Learning representations by back-propagating errors, *Nature* **323**: 533–536.

Shidara, M., Kawano, K., Gomi, H. and Kawato, M. (1993) Inverse-dynamics model eye movement control by purkinje cells in the cerebellum, *Nature* **365**(6441) 50–52.

Soechting, J. and Roberts, W. (1975) Transfer characteristics between emg activity and muscle tension under isometric conditions in man, *Journal of Physiology* **70**: 779–793.

Suzuki, R. and Suematsu, T. (1969) Pattern recognition of multi-channel mioelectric signals by learning method, *Japanese Journal of Medical Electronics and Biological Engineering* **7**(1): 47–48. (in Japanese).

Uno, Y., Kawato, M. and Suzuki, R. (1989) Formation and control of optimal trajectory in human multijoint arm movement: minimum torque-change model, *Biological Cybernetics* **61**: 89–101.

Uno, Y., Suzuki, R. and Kawato, M. (1989) Minimum-muscle-tension-change model which reproduces human arm movement, *Proceedings of the 4th Symposium on Biological and Physiological Engineering* pp. 299–302. (in Japanese).

Wada, Y. and Kawato, M. (1992) A new information criterion combined with cross-validation method to estimate generalization capability, *Systems and Computers in Japan* **23**: 92–104.

Winters, J. M. (1990) Hill-based muscle models : A systems engineering perspective, *in* J. M. Winters and S. L.-Y. Woo (eds), *Multiple Muscle Systems*, Springer-Verlag, New York, pp. 69–93.

Wood, J., Meek, S. and Jacobsen, S. (1989) Quantitation of human shoulder anatomy for prosthetic arm control–II.anatomy matrices, *J. Biomechanics* **22**(4): 309–325.